

Static and dynamic magnetic properties of sputtered Fe-Ga thin films

Daniel B. Gopman¹, Vimal Sampath², Hasnain Ahmad³, Supriyo Bandyopadhyay³, and Jayasimha Atulasimha^{2,3}

¹Materials Science & Engineering Division, National Institute of Standards and Technology, Gaithersburg, MD, 20899 USA

²Mechanical and Nuclear Engineering, Virginia Commonwealth University, Richmond, VA, 23284 USA

³Electrical and Computer Engineering, Virginia Commonwealth University, Richmond, VA, 23284 USA

We present measurements of the static and dynamic properties of polycrystalline iron-gallium films, ranging from 20 nm to 80 nm and sputtered from an $\text{Fe}_{0.8}\text{Ga}_{0.2}$ target. Using a broadband ferromagnetic resonance setup in a wide frequency range, perpendicular standing spin-wave resonances were observed with the external static magnetic field applied in-plane. The field corresponding to the strongest resonance peak at each frequency is used to determine the effective magnetization, the g -factor and the Gilbert damping. Furthermore, the dependence of spin-wave mode on field-position is observed for several frequencies. The analysis of broadband dynamic properties allows determination of the exchange stiffness $A = (18 \pm 4) \text{ pJ/m}$ and Gilbert damping $\alpha = 0.042 \pm 0.005$ for 40 nm and 80 nm thick films. These values are approximately consistent with values seen in epitaxially grown films, indicating the potential for industrial fabrication of magnetostrictive FeGa films for microwave applications.

I. INTRODUCTION

RECENT interest in the control of nanoscale magnetism by voltage, either by the voltage-control of magnetic anisotropy phenomena [1]–[3] or through strain based switching [4]–[8] in magnetoelectric composites. In the latter case, a nanomagnet is placed in elastic contact with a piezoelectric element, enabling voltage tuning of the strain field generated in the piezoelectric element and partially or fully transferred to the magnetostrictive nanomagnet. These voltage-controlled applications are motivated by a technological interest to identify methods for controlling the magnetism of nanoscale magnetic elements for magnetic memory and logic applications [9]–[11] with lower energy cost than contemporary solutions involving generating local Oersted fields [12], [13] or torques from spin-polarized electric currents [14]–[16].

A series of new experiments have shown the possibility of strain-mediated switching in Co [17]–[19] and FeGa-alloy based nanomagnets [20]. While transition metal ferromagnets (Fe, Co, Ni) exhibit relatively modest bulk magnetostriction coefficients ($\sim 10^{-5}$), binary and ternary alloys such as $\text{Fe}_{0.81}\text{Ga}_{0.19}$ (Galfenol) and $\text{Tb}_{0.3}\text{Dy}_{0.7}\text{Fe}_2$ (Terfenol-D) exhibit magnetostriction coefficients nearly ten times higher for particular stoichiometric compositions [21], [22]. Such large magnetostriction would enable highly reliable, voltage induced switching of magnetization when combined with a piezoelectric element. In order to assess the switching speed of a technology based on these materials, it is critical to evaluate the dynamic magnetic properties (including Gilbert damping and the ferromagnetic exchange constant) for films with relevant thicknesses for device fabrication (e.g. sub-100 nm). To this end, we have fabricated a series of FeGa alloy films using room temperature, DC magnetron sputtering. The films range from 20 nm to 80 nm, enabling us to evaluate the chemical, physical and static and dynamic magnetic properties across a wide thickness range. We find that while the magnetization is reduced compared to bulk and single crystalline specimens, the Gilbert damping and

exchange stiffness values are comparable to those obtained in molecular-beam epitaxially grown films, an encouraging prospect for industrial fabrication of devices based on FeGa thin films.

II. SAMPLE PREPARATION

SAMPLES were grown by DC magnetron sputtering onto thermally oxidized Si(001) substrate wafers in a multi-target chamber with a base pressure of less than 4×10^{-7} Torr and at ambient temperature. Each sample consists of a 3 nm Ta adhesion layer, followed by a 12 nm thick Cu buffer layer, reported to enhance the magnetostrictive quality of polycrystalline FeGa thin films by encouraging a (110) crystalline texture along the growth direction. [23] Subsequently, FeGa

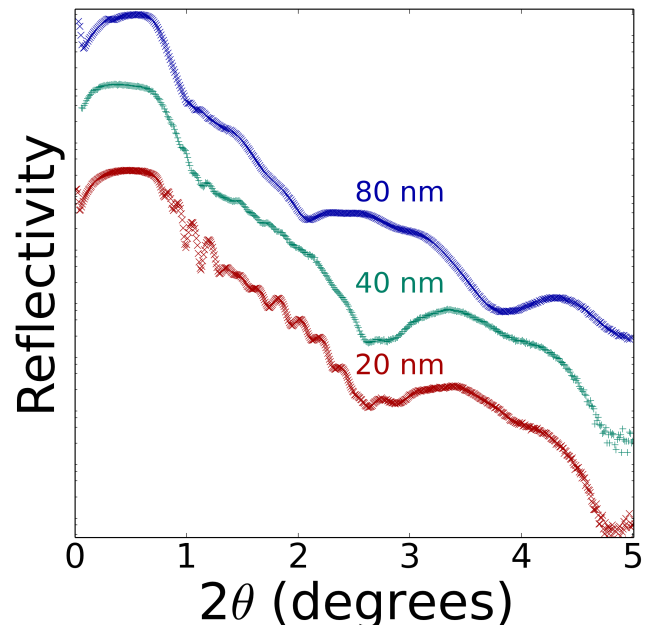


Fig. 1. X-ray reflectivity results showing intensity versus 2θ angle for samples with three nominal FeGa thicknesses. Intensity curves are vertically offset from one another.

films of nominal thickness $\delta = 20$ nm, 40 nm or 80 nm were overlaid on top of the Cu buffer, and each film was subsequently capped by a 5 nm thick Ta protective layer. The target material used to grow the FeGa layers was obtained with a stoichiometry of 81% Fe and 19% Ga. Energy-dispersive x-ray spectroscopy from a scanning electron microscope was used to quantify the atomic fraction of Fe to Ga in each sample, showing a dispersion in Ga content from 15% to 25%. It has been demonstrated that Ga concentration variation affects the magnetic properties, including magnetostriction, saturation magnetization and coercivity, strongly and the observed spread is consistent with films sputtered from stoichiometric targets. [29]–[33]. This may also influence the dynamic properties to be discussed below.

THE layer thicknesses and interfacial roughnesses were estimated by x-ray reflectometry studies using a Rigaku SmartLab X-Ray Diffractometer with a Cu $K\alpha$ x-ray source and a Ge(220) 2 bounce monochromator on the incident beam ahead of our sample [24]. In particular, Fig. 1 shows the three x-ray reflectivity spectra for each sample in the series. While the frequency of the oscillation corresponding to the FeGa thickness fringes is increasing with thickness along the sample series, the estimated interfacial roughness increases from 2.3 nm to 3.0 nm, as can be seen by the reduced amplitude of the thickness fringes going from 20 nm to 80 nm. The estimated thicknesses and roughness values are listed in Table I. This structural information will be useful for the interpretation of the static and dynamic magnetic properties below.

EACH sample was spin-coated with approximately 150 nm of polymethyl methacrylate photoresist in preparation for magnetic measurements. This enabled the minimization of sample contamination during cleaving into 3 mm \times 4 mm rectangular pieces for magnetization measurements. This also served as a protective barrier against electrical shorting of the center line from the ground plane of microstrip ferromagnetic resonance spectroscopy measurements.

III. STATIC AND DYNAMIC MAGNETIC PROPERTIES OF FE/GA THIN FILMS

MAGNETIZATION and magnetic coercivity were measured with the help of a Micro Sense vibrating sample magnetometer [24]. Applied in-plane magnetic field versus magnetization hysteresis curves were obtained for the three samples and are shown in Fig. 2. All samples approach saturation under a moderate in-plane field (≤ 20 mT) with a saturation induction of approximately 1.5 T. The saturation magnetization values are markedly lower in comparison to epitaxially grown FeGa films as well as bulk samples by more than 10 %, which may indicate a limitation in sputtered, polycrystalline FeGa films. [23], [25] Furthermore, the magnetic coercive field increases along with the FeGa thickness: 1.5 mT \pm 0.3 mT ($\delta=20$ nm); 6.5 mT \pm 0.3 mT ($\delta=40$ nm) and 14.5 mT \pm 0.3 mT ($\delta=80$ nm). Uncertainty in the coercivity comprises the uncertainty in the precision of the measured field values. The increase in coercivity is also accompanied by an increase of the saturation field, which for the 80 nm thick

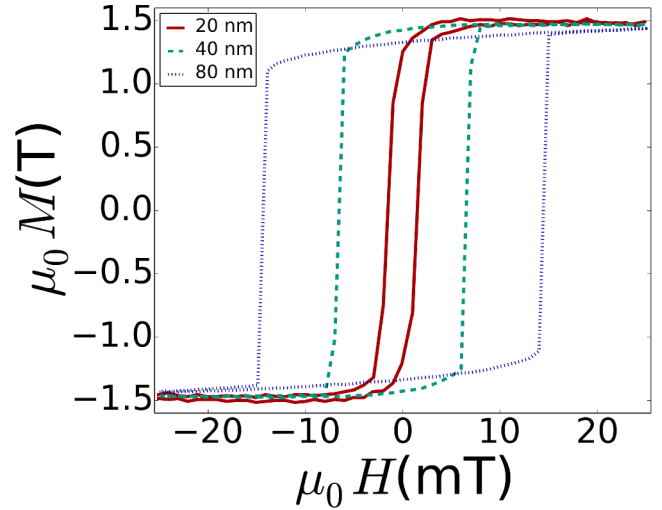


Fig. 2. Magnetization versus applied field hysteresis curves for samples with three nominal FeGa thicknesses.

sample exceeds the maximum field in the Fig. 2 plotting canvas (± 25 mT). The increase in coercive field is consistent with the roughening of the sputtered FeGa layer with thickness noticed first in the x-ray reflectivity. The relationship between Ga content (high) and saturation magnetization (low) and magnetic coercivity (low) is consistent with previous studies of polycrystalline FeGa alloy films. [29], [32] Moreover, this is also consistent with the development of in-plane magnetic anisotropies, which will be shown in the following section.

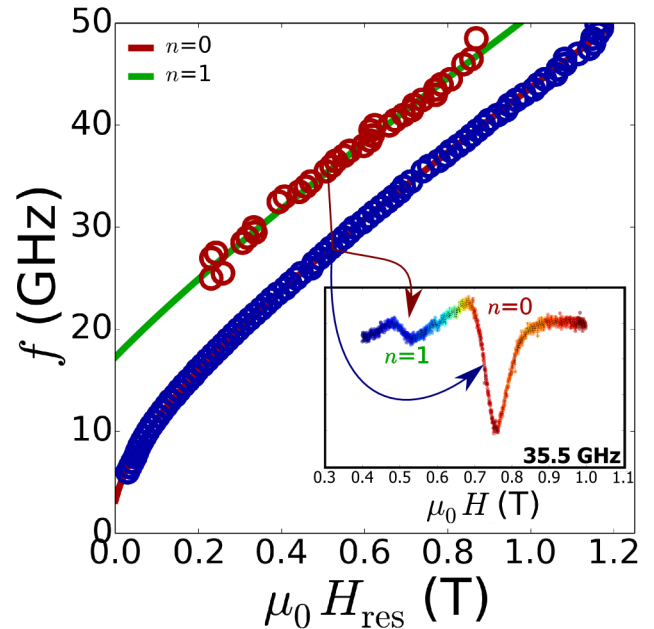


Fig. 3. The uniform mode ferromagnetic resonance frequency versus field (blue circles) and red best-fit line and first PSSW mode frequency versus field (red circles) and green best-fit line. Inset: ferromagnetic resonance spectra at a single frequency $f = 35.5$ GHz showing the two absorption modes extracted for several frequencies.

TABLE I
COMPARISON OF STATIC AND DYNAMIC PROPERTIES OF FeGa THIN FILMS.

Fe _{1-x} Ga _x δ (nm)	σ_{rms} (nm)	x (%)	$\mu_0 H_C$ (mT)	$\mu_0 M_s$ (T)	$\mu_0 H_{\text{cub}}$ (mT)	α	$\mu_0 \Delta H_0$ (mT)	A_{ex} (pJ/m)
21.2 \pm 0.5	2.3 \pm 0.1	25 \pm 4	1.5 \pm 0.3	1.47 \pm 0.04	1 \pm 1	0.012 \pm 0.001	6.7 \pm 0.5	-
42.3 \pm 0.5	2.6 \pm 0.1	20 \pm 2	6.5 \pm 0.3	1.53 \pm 0.02	11 \pm 1	0.038 \pm 0.001	35 \pm 1	18 \pm 4
80.7 \pm 0.5	3.1 \pm 0.1	18 \pm 1	14.5 \pm 0.3	1.56 \pm 0.02	10 \pm 1	0.047 \pm 0.001	44 \pm 1	17 \pm 5
21 [26]	-	19	2.5	1.7	30	0.017	1.8	-
65 [25]	-	20	-	1.76	11.4	-	-	16

THE dynamical properties of the FeGa films were studied using broadband ferromagnetic resonance spectroscopy. At fixed rf excitation frequencies, we sweep an applied in-plane magnetic field and record the position of Lorentzian-shaped absorption modes. A low frequency excitation field ($f = 277$ Hz, $B_{\text{pk}} = 1$ mT) is superposed onto the dc magnetic field for improved signal-to-noise using lock-in detection of the differential absorption. As shown in the inset to Fig. 3, we observe a high-field, large amplitude uniform mode and one additional lower-field, smaller amplitude mode. At each frequency, we fit the data shown in the inset to the sum of two derivative Lorentzian absorption lines, from which we obtain the resonance field $\mu_0 H_{\text{res}}$ and the linewidth $\mu_0 \Delta H$ for each mode. The frequency dependence of the high-field, large amplitude ferromagnetic resonance field and its linewidth are related to the various dynamic properties of FeGa (magnetic anisotropy, spectroscopic g -factor and Gilbert damping). The additional modes originates in perpendicular standing spin-wave (PSSW) modes created by surface pinning at the top (and/or bottom) interfaces and quantized through the thickness of the FeGa film. Their magnetic field separation from the uniform mode is related to the exchange stiffness. We evaluate the mode dependence of the first PSSW mode at a series of rf frequencies to determine the exchange constant, A . [27]

THE Kittel equation for ferromagnetic resonance governs the relationship between microwave excitation frequency f and resonant applied magnetic field for fields applied within the thin film plane:

$$\left(\frac{2\pi f}{\gamma\mu_0}\right)^2 = (H_{\text{res}} + H_{\text{cub}} + H_{\text{ex}}) \times \quad (1)$$

$$(H_{\text{res}} + H_{\text{cub}} + M_{\text{eff}} + H_{\text{ex}}), \quad (2)$$

where $\gamma = g\mu_B/\hbar$ is the gyromagnetic ratio, g is the g -factor, μ_B is the Bohr magneton, \hbar is the reduced Planck constant, μ_0 is the vacuum permeability, H_{cub} is the cubic anisotropy, M_{eff} is the effective magnetization (comprising the saturation magnetization minus uniaxial anisotropy field) and $\mu_0 H_{\text{ex}} = 2A(n\pi/\delta)^2/M_S$ is the exchange field of the n -th PSSW mode for film thickness δ , saturation magnetization M_S and exchange constant A . The frequency dependence of the ferromagnetic resonance linewidth is fit to a line to determine the internal Gilbert damping (α) and linewidth broadening due to inhomogeneities in the magnetic film (ΔH_0):

$$\Delta H = \frac{4\pi\alpha f}{\gamma\mu_0} + \Delta H_0. \quad (3)$$

BY fitting the data in Fig. 3 (and the corresponding data for the 20 nm and 80 nm samples) to the two Eqns. (2)&(3), we can extract values for the dynamic properties of each film. These values are collected along with the static magnetic properties and the structural properties into Table I. We note that for the 20 nm film, it was not possible to observe any PSSW modes, due in part to the large exchange field associated with the relatively thinner film and possibly reduced surface pinning required for the development of PSSW modes. Notably, for samples with 40 nm thickness and 80 nm thickness, the values for the cubic anisotropy field (11 mT \pm 1 mT) and the exchange constant (18 pJ/m \pm 4 pJ/m) fall within the range of previously recorded values for single crystalline Galfenol thin films. [25], [26] Uncertainty in our bestfit parameters herein comprises the standard uncertainty from a leastsquares fit to Eq. 2, and the uncertainty in measured quantities for the saturation magnetization and film thickness.

WE note an interesting trend in the ferromagnetic resonance linewidth versus frequency trend, shown in Fig. 4. While the general increase in inhomogeneous broadening is consistent with the higher roughness and larger coercivity seen in the 40 nm and 80 nm films, respectively, the nearly three-fold increase in the Gilbert damping between the 20 nm film and the 40 nm film is statistically significant. Compared to a recent study on an epitaxially grown 21-nm thick Galfenol film, in which the Gilbert damping (0.017) is comparable to the damping measured in our 20 nm thick film (0.012), there may be a meaningful thickness dependence to the damping in FeGa alloys [26]. Since the ferromagnetic resonance linewidth used to estimate the Gilbert damping was measured under in-plane applied fields, a significant two-magnon linewidth contribution through large ΔM_{eff} could be the source of increased damping. Future studies with experimental setups capable of applying saturating out-of-plane magnetic fields could be aimed at eliminating the contribution of two-magnon scattering from the thickness-dependence of the Gilbert damping. [28]

IV. CONCLUSION

WE have investigated the static and dynamic magnetic properties of a series of polycrystalline FeGa films sputter deposited at room temperature. The comparable exchange stiffness to epitaxially grown films is promising for processing continuous films into patterned, single domain nanoelements. Furthermore, the large magneto-mechanical coupling and Gilbert damping as low as 0.012 is competitive for high-speed nanodevices when compared to a magnetostrictive alloy like Terfenol-D ($\alpha \geq 0.1$). [27] We note that

accounting for the spread in stoichiometry remains a challenge for sputtered Galfenol films from a single target. It appears that this may be resolved by optimized co-deposition from target materials with distinct Fe-to-Ga ratio [30]. Also there is a clear need to mitigate the interfacial roughness (and corresponding coercive field and inhomogeneous broadening increases with film thickness). Nevertheless, we note that the results presented for the 40 nm and the 80 nm films presented in Table I show reasonable agreement with literature values for the expected cubic anisotropies, Gilbert damping and exchange stiffness. In summary, there appears to be a large variation in the Gilbert damping due to thickness, Ga content and possible process variations. Future studies could be aimed at identifying means to reduce the apparent dissipative mechanisms, which will enable the use of ultrathin Galfenol nanostructures in low-energy, fast, magnetic storage and logic applications.

ACKNOWLEDGMENT

V.S, J.A, H.A, S.B acknowledge NSF SHF-Small Grant CCF-1216614. J. A. and V.S acknowledge support from NSF CAREER grant CCF-1253370. D.B.G. acknowledges the National Institute of Standards and Technology, Center for Nanoscale Science and Technology Nanofabrication Facility under Project No. N12.0033.06.

REFERENCES

- [1] C. Grezes, F. Ebrahimi, J. G. Alzate, X. Cai, J. A. Katine, J. Langer, B. Ocker, P. K. Amiri, and K. L. Wang, "Ultra-low switching energy and scaling in electric-field-controlled nanoscale magnetic tunnel junctions with high resistance-area product," *Applied Physics Letters*, vol. 108, no. 1, 2016.
- [2] D. Chiba, M. Yamanouchi, F. Matsukura, and H. Ohno, "Electrical manipulation of magnetization reversal in a ferromagnetic semiconductor," *Science*, vol. 301, no. 5635, pp. 943–945, 2003.
- [3] D. Chiba, M. Sawicki, Y. Nishitani, Y. Nakatani, F. Matsukura, and H. Ohno, "Magnetization vector manipulation by electric fields," *Nature*, vol. 455, no. 7212, pp. 515–518, 2008.
- [4] J. Atulasimha and S. Bandyopadhyay, "Bennett clocking of nanomagnetic logic using multiferroic single-domain nanomagnets," *Applied Physics Letters*, vol. 97, no. 17, 2010.

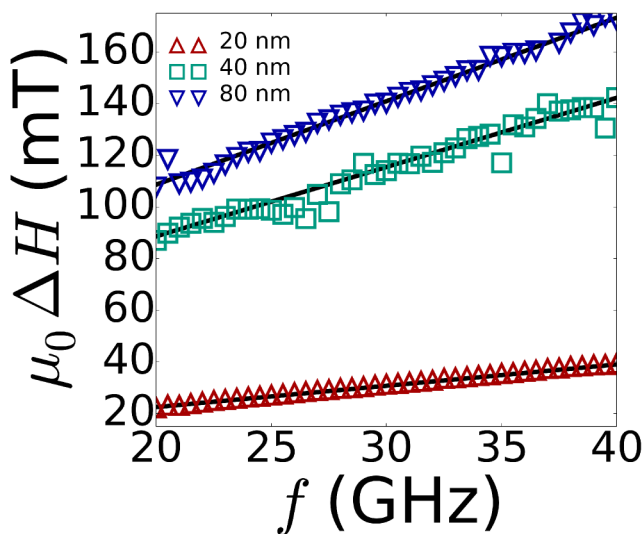


Fig. 4. Ferromagnetic resonance linewidth versus uniform mode frequency for samples with three nominal FeGa thicknesses.

- [5] K. Roy, S. Bandyopadhyay, and J. Atulasimha, "Hybrid spintronics and straintronics: A magnetic technology for ultra low energy computing and signal processing," *Applied Physics Letters*, vol. 99, no. 6, 2011.
- [6] N. Tiercelin, Y. Dusch, A. Klimov, S. Giordano, V. Preobrazhensky, and P. Pernod, "Room temperature magnetoelectric memory cell using stress-mediated magnetoelastic switching in nanostructured multilayers," *Applied Physics Letters*, vol. 99, no. 19, 2011.
- [7] J. Z. Cui, J. L. Hockel, P. K. Nordeen, D. M. Pisani, C. Y. Liang, G. P. Carman, and C. S. Lynch, "A method to control magnetism in individual strain-mediated magnetoelectric islands," *Applied Physics Letters*, vol. 103, no. 23, 2013.
- [8] M. Buzzi, R. V. Chopdekar, J. L. Hockel, A. Bur, T. Wu, N. Pilet, P. Warnicke, G. P. Carman, L. J. Heyderman, and F. Nolting, "Single domain spin manipulation by electric fields in strain coupled artificial multiferroic nanostructures," *Physical Review Letters*, vol. 111, no. 2, 2013.
- [9] R. P. Cowburn and M. E. Welland, "Room temperature magnetic quantum cellular automata," *Science*, vol. 287, no. 5457, pp. 1466–1468, 2000.
- [10] S. Salahuddin and S. Datta, "Interacting systems for self-correcting low power switching," *Applied Physics Letters*, vol. 90, no. 9, 2007.
- [11] S. Bandyopadhyay and M. Cahay, "Electron spin for classical information processing: a brief survey of spin-based logic devices, gates and circuits," *Nanotechnology*, vol. 20, no. 41, 2009.
- [12] A. Ney, C. Pampuch, R. Koch, and K. H. Ploog, "Programmable computing with a single magnetoresistive element," *Nature*, vol. 425, no. 6957, pp. 485–487, 2003.
- [13] M. T. Alam, M. J. Siddiq, G. H. Bernstein, M. Niemier, W. Porod, and X. S. Hu, "On-chip clocking for nanomagnet logic devices," *Ieee Transactions on Nanotechnology*, vol. 9, no. 3, pp. 348–351, 2010.
- [14] J. C. Slonczewski, "Current-driven excitation of magnetic multilayers," *Journal of Magnetism and Magnetic Materials*, vol. 159, no. 1-2, pp. L1–L7, 1996.
- [15] D. C. Ralph and M. D. Stiles, "Spin transfer torques," *Journal of Magnetism and Magnetic Materials*, vol. 320, no. 7, pp. 1190–1216, 2008.
- [16] L. Q. Liu, C. F. Pai, Y. Li, H. W. Tseng, D. C. Ralph, and R. A. Buhrman, "Spin-torque switching with the giant spin hall effect of tantalum," *Science*, vol. 336, no. 6081, pp. 555–558, 2012.
- [17] N. D'Souza, M. S. Fashami, S. Bandyopadhyay, and J. Atulasimha, "Experimental clocking of nanomagnets with strain for ultralow power boolean logic," *Nano Letters*, vol. 16, no. 2, pp. 1069–1075, 2016.
- [18] V. Sampath, N. D'Souza, D. Bhattacharya, G. M. Atkinson, S. Bandyopadhyay, and J. Atulasimha, "Acoustic-wave-induced magnetization switching of magnetostrictive nanomagnets from single-domain to non-volatile vortex states," *Nano Letters*, vol. 16, no. 9, pp. 5681–5687, 2016.
- [19] V. Sampath, N. D'Souza, G. M. Atkinson, S. Bandyopadhyay, and J. Atulasimha, "Experimental demonstration of acoustic wave induced magnetization switching in dipole coupled magnetostrictive nanomagnets for ultralow power computing," *Applied Physics Letters*, vol. 109, no. 10, pp. 123–126, 2016.
- [20] H. Ahmad, J. Atulasimha, and S. Bandyopadhyay, "Reversible strain-induced magnetization switching in fega nanomagnets: Pathway to a rewritable, non-volatile, non-toggle, extremely low energy straintronic memory," *Scientific Reports*, vol. 5, 2015.
- [21] M. Wun-Fogle, J. B. Restorff, and A. E. Clark, "Magnetomechanical coupling in stress annealed fe-ga and fe-al alloys," in *INTERMAG 2006 - IEEE International Magnetism Conference*, May 2006, pp. 679–679.
- [22] T. A. Duenas and G. P. Carman, "Large magnetostrictive response of terfenol-d resin composites (invited)," *Journal of Applied Physics*, vol. 87, no. 9, pp. 4696–4701, 2000.
- [23] J. Weston, A. Butera, T. Lograsso, M. Shamsuzzoha, I. Zana, G. Zangari, and J. Barnard, "Fabrication and characterization of Fe₈₁Ga₁₉ thin films," *IEEE TRANSACTIONS ON MAGNETICS*, vol. 38, no. 5, 1, pp. 2832–2834, SEP 2002.
- [24] Certain commercial equipment, instruments, or materials are identified in this paper in order to specify the experimental procedure adequately. Such identification is not intended to imply recommendation or endorsement by the National Institute of Standards and Technology, nor is it intended to imply that the materials or equipment identified are necessarily the best available for the purpose.
- [25] S. Tacchi, S. Fin, G. Carlotti, G. Gubbiotti, M. Madami, M. Barturen, M. Marangolo, M. Eddrief, D. Bisero, A. Rettori, and M. G. Pini, "Rotatable magnetic anisotropy in a fe_{0.8}ga_{0.2} thin film with stripe domains: Dynamics versus statics," *Physical Review B*, vol. 89, no. 2, 2014.

- [26] D. E. Parkes, L. R. Shelford, P. Wadley, V. Holy, M. Wang, A. T. Hindmarch, G. van der Laan, R. P. Campion, K. W. Edmonds, S. A. Cavill, and A. W. Rushforth, "Magnetostrictive thin films for microwave spintronics," *Scientific Reports*, vol. 3, 2013.
- [27] D. B. Gopman, J. W. Lau, K. P. Mohanchandra, K. Wetzlar, and G. P. Carman, "Determination of the exchange constant of $\text{tb}_0.3\text{dy}_0.7\text{fe}_2$ by broadband ferromagnetic resonance spectroscopy," *Physical Review B*, vol. 93, no. 6, 2016.
- [28] R. Arias and D. L. Mills, "Extrinsic contributions to the ferromagnetic resonance response of ultrathin films," *Phys. Rev. B*, vol. 60, pp. 7395–7409, Sep 1999.
- [29] A. Javed, T. Szumiata, N. Morley, and M. Gibbs, "An investigation of the effect of structural order on magnetostriction and magnetic behavior of fega alloy thin films," *Acta Materialia*, vol. 58, no. 11, pp. 4003 – 4011, 2010.
- [30] A. Javed, N. A. Morley, and M. R. J. Gibbs, "Thickness dependence of magnetic and structural properties in $\text{fe}_{80}\text{ga}_{20}$ thin films," *Journal of Applied Physics*, vol. 107, no. 9, p. 09A944, 2010.
- [31] A. Javed, N.A. Morley, "Structure, magnetic and magnetostrictive properties of as-deposited fega thin films," *Journal of Magnetism and Magnetic Materials*, vol. 321, no. 18, pp. 2877–2882, 2009.
- [32] J. Atulasimha, A. B. Flatau, and J. R. Cullen, "Analysis of the effect of gallium content on the magnetomechanical behavior of single-crystal fega alloys using an energy-based model," *Smart Materials and Structures*, vol. 17, no. 2, p. 025027, 2008.
- [33] A. E. Clark, J. B. Restorff, M. Wun-Fogle, T. A. Lograsso, and D. L. Schlagel, "Magnetostrictive properties of body-centered cubic fe-ga and fe-ga-al alloys," *IEEE Transactions on Magnetics*, vol. 36, no. 5, pp. 3238–3240, 2000.